Vision out of the corner of the eye

M.P.S. To [a,*], B.C. Regan [b], Dora Wood [b], J.D. Mollon [b]

[a] Department of Physiology, Development and Neuroscience, University of Cambridge, Downing Street, Cambridge CB2 3EG, UK
[b] Department of Experimental Psychology, University of Cambridge, Downing Street, Cambridge CB2 3EB, UK

ABSTRACT

The margin of the temporal visual field lies more than 90° from the line of sight and is critical for detecting incoming threats and for balance and locomotive control. We show (i) contrast sensitivity beyond 70° is higher for moving stimuli than for stationary, and in the outermost region, only moving stimuli are visible; (ii) sensitivity is highest for motion in directions near the vertical and horizontal axes and is higher for forward than for backward directions; (iii) the former anisotropy arises early in the visual pathway; (iv) thresholds for discriminating direction are lowest for upward and downward motion.

Crown Copyright © 2010 Published by Elsevier Ltd. All rights reserved.

1. Introduction

1.1. Vision at the temporal margin of the visual field

At the foremost margin of the retina, near the *ora serrata*, the ganglion cells are reduced to a single layer, and are 'mostly separated by long gaps, being usually grouped in twos or threes' (Polyak, 1941). Polyak himself judged this retinal region to be of 'small physiological interest'. Yet there are two reasons why the extreme margin of the retina deserves further attention.

First, the very sparseness of ganglion cells is a positive attraction to the psychophysicist. We now know that the central regions of the retina are tessellated by at least 20 distinct types of ganglion cell; and it has become untenable to distinguish just two functional channels, magnocellular and parvocellular (Crook et al., 2008; Dacey, Peterson, Robinson, & Gamlin, 2003; Yamada, Bordt, & Marshak, 2005). In the central field, therefore, the psychophysical isolation of a single channel will always be challenging. But the sparse and single layer of ganglion cells in the extreme periphery hints that the number of channels is very small, possibly as low as one. The present paper attempts a very preliminary characterization of vision mediated by this part of the retina.

Second, the nasal margin of the retina is of clear functional importance. It corresponds to the extreme temporal field, which is the first retinal region to be stimulated by stimuli entering the field from behind, stimuli that might represent a threat. We may expect this retinal margin to act as a sentinel, detecting sudden changes and movements and triggering foveation towards, or avoidance of, stimuli entering the field (Porter, 1902). The far periphery is also essential in maintaining balance, both when the observer is stationary and when he or she is in locomotion. If the observer is fixating the point to which he is moving, the velocity of flow patterns is greatest at 90° from the line of sight (Gibson, 1947; Grindley, 1942). Motion in this region has the most prominent effect in generating vection – the illusion of self-motion in a stable environment (Pavard, Berthoz, & Lestienne, 1976): stationary observers can experience vection when the central 120° of their visual field are occluded (Brandt, Dichgans, & Koenig, 1973). Similarly, Bessou, Severac Cauquil, Dupui, Montoya, and Bessou (1999) have shown that the far periphery is critical in stabilizing the head and body. These postural adjustments can be very rapid, and it may be relevant that Palmer and Rosa (2006) have reported in a callitrichid primate that the representation of the monocular crescent in the medial temporal lobe draws its predominant input direct from V1 rather than indirectly via V2.

1.2. Psychophysics at the edge of the visual field

Only a few psychophysical studies have examined visual performance at the lateral margin of the field. In man, the temporal field extends to more than 100° from the line of sight (Druault, 1898; Hartridge, 1919; Purkinje, 1825; Young, 1801). At these extreme eccentricities, only bright stimuli are visible, owing to the reduction in the effective area of the pupil: photographic measurements by Jay (1962) show that the effective area of the pupil – compared to its area when photographed along the line of sight – falls to 0.1 at an eccentricity of 98° and 0.05 at about 100°.

In his classic paper of 1875, Sigmund Exner claimed that in the outermost part of the lower visual field there was a region where he experienced a pure sensation of motion without form or color.

* Corresponding author.
E-mail address: to@cantab.net (M.P.S. To).

It may seem almost funny (*fast komisch*), he wrote, that one can see motion without a moving object, but that was the only way to describe his sensation (Exner, 1875, p. 163). His words anticipate the descriptions given by patients who have suffered injuries to the primary visual cortex and who are shown an object moving within their blind field (Azzopardi & Cowey, 1998; Riddoch, 1917). Thus, for Exner the far periphery was an organ specialized for the perception of motion.

There have been many subsequent investigations of peripheral sensitivity to motion (Hulk & Rempt, 1984; Koenderink, Bouman, Bueno de Mesquita, & Slappendel, 1978; McKee & Nakayama, 1984; Sharpe, 1974) and to temporal modulation (Navarro, Artal, & Williams, 1993; Pointer & Hess, 1989; Robson & Graham, 1981; van Ness, Koenderink, Nas, & Bouman, 1967). However, very few studies have examined sensitivity to motion at eccentricities beyond 50–60°; and psychophysical measurements at the edge of the field certainly require dedicated, trained observers, owing to the 90-degree separation between direction of fixation and the direction of attention.

Noorlander, Koenderink, den Ouden, and Edens (1983) showed that spatio-temporal chromatic modulation could be detected at eccentricities as great as 90°. For a range of eccentricities from 83° to 105°, Mollon, Regan, and Bowmaker (1998) measured temporal contrast sensitivity at 18 Hz. The stimulus was a bar subtending 1 by 8.6° and it consisted of yellow and blue components flickered in counterphase, which allowed an approximation to a silent substitution for rods. Contrast sensitivity declined monotonically over the range tested: there was no discontinuity that might be associated with the mysterious cone rim that is present at the retinal margin (Greeff, 1900; Williams, 1991).

In the present study, we measured spatial contrast sensitivity functions for detecting stationary and moving gratings in the far periphery. We show formally that only moving gratings are visible at the temporal margin of the field. We demonstrate that there are strong anisotropies in sensitivity for detecting Gabor patches moving in different directions and that these anisotropies are reversed for plaid stimuli. We also report thresholds for discriminating the direction of moving Gabors.

2. Experiment 1

In Experiment 1, we show that thresholds for moving targets are lower than for stationary ones in the extreme peripheral field; and that at the limit of the field, only moving stimuli are detectable. A preliminary report of this experiment has been published (Mollon & Regan, 1999).

2.1. Methods

2.1.1. Set-up

The observer was seated so that his or her left eye was level with the centre of the monitor screen placed 1.6 m from the eye. A wax dental impression was used to stabilize head position. The right eye was covered by a patch. Apart from the display, the room was dark and the observer faced a three-sided black booth, which served to minimize light scattered from the display (see Fig. 1).[1] A fixation stimulus on the far wall of the booth could be adjusted laterally in position in order to vary the eccentricity of the target: the fixation stimulus subtended 0.5° and consisted of a dim white square region with a central green disk, in the centre of which was a black cross. The observer was instructed to fixate the centre of the cross; lapses of fixation were revealed to him or her by the appearance of a colored after-image against the white area.
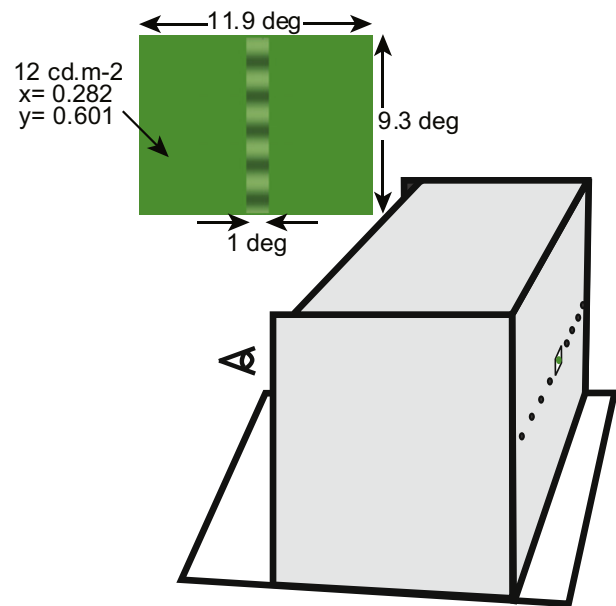

Fig. 1. Stimulus display and viewing arrangement for Experiment 1. Observers were seated with their left eye level with the centre of a calibrated monitor, located 1.6 m from the test eye. A mouth-bite was used to stabilize head position. The observer viewed a fixation light visible through holes at the back of the black booth.

2.1.2. Stimuli

Stimuli were presented on a Sony Colour Graphics monitor (GDM-1936) using a Cambridge Research Systems graphics card (VSG 2/3). The frame rate was 70 Hz. The test stimulus was a vertical strip, which could be modulated at different spatial frequencies and contrasts (see Fig. 1). To avoid detection of the modulation by scattered light, the test stimulus was embedded in a larger, illuminated region subtending 11.9 by 9.3°. The luminance of the background and the mean luminance of the stimulus were both 12 cd m^{-2}. Both the background and the stimulus were green, with CIE$_{1931}$ coordinates of 0.282, 0.600. Calibrations were performed with a PhotoResearch 650 spectroradiometer.

There were two main experimental conditions: in one condition, the sinusoidal grating moved either up or down the strip at 9.3° per second for 1.5 s. The direction of motion was random from trial to trial. In the other condition, the spatial modulation was presented without displacement for the same interval. In both cases, the modulation was Gaussian-filtered in time, with a standard deviation of 300 ms, so that there was no detectable transient at onset.

2.1.3. Procedure

The task was a two-interval temporal forced choice: the modulation of the vertical strip was present in only one of two intervals and the observer responded 'first' or 'second' by means of pushbuttons. A warning tone preceded each interval. Contrast was altered according to a staircase procedure, being increased after any incorrect response and reduced after two consecutive correct ones: this rule tracks the contrast at which the observer is 71% correct (Wetherill & Levitt, 1965). Two independent staircases were randomly interleaved.

At each of 11 eccentricities, ranging from 72.5° to 97.5° from the line of sight, we measured contrast thresholds for moving and for stationary gratings at eight spatial frequencies. On the basis of pilot studies, we tested spatial frequencies in the range 0.11–1.22 cycles per degree of visual angle. Within an experimental run, spatial frequencies were tested in random order; different eccentricities were tested in separate runs, also randomised. Each threshold was measured four times in separate sessions.

---

[1] For interpretation of color in Figs. 1, 4, 6, 8 and 9, the reader is referred to the web version of this article.

2.1.4. Observers

The observers were the authors JM (male) and DW (female). Both had extensive experience in maintaining central fixation while judging peripheral stimuli.

2.2. Results

The first seven panels of Fig. 2a show the contrast sensitivity functions obtained for JM in the range of eccentricities 72.5–87.5° from the line of sight. Solid points show thresholds for moving gratings and open circles show those for stationary modulations. The thresholds shown are averages from four separate runs. For conditions where the observer was unable to set a threshold on at least one run, no data point is plotted. The curves fitted to the data are third-order polynomials and are not intended to have theoretical significance.

As eccentricity increases, the maximum sensitivity falls for both moving and stationary gratings, but for all eccentricities and all spatial frequencies, the observer's sensitivity is systematically higher for moving than for stationary gratings. For moving gratings, the peaks of the fitted curves all lie between 0.3 and 0.4 cycles per degree, whereas maximum sensitivity for stationary gratings usually lies at a lower spatial frequency.

The final panel of Fig. 2a shows the thresholds obtained for moving gratings at 90°, 92.5° and 95° eccentricity. At these eccentricities, there does exist a region where the stationary modulation is virtually invisible. The only exception was for spatial frequency = 0.11 cycles per degree and eccentricities 90 and 92.5, where (very low) log contrast sensitivities of 0.038 and 0.122 were recorded. Movement sensitivity for JM extends to 95°. The final pocket of motion sensitivity remains in a region close to 0.3 cycles per degree. Ancillary measurements for this observer showed that sensitivity is not narrowly tuned for *temporal* frequency: it is spatial frequency that is critical.

Fig. 2b shows spatial contrast sensitivity functions for DW for a similar range of eccentricities. As in the case of JM, DW's sensitivity for moving gratings is substantially higher than for static ones; and (with the one exception of .11 cycles per degree at 87.5° eccentricity) she cannot detect static gratings at eccentricities of 85° and higher. The estimated peak sensitivities for moving stimuli lie in the range 0.1–0.35 cycles per degree, a slightly lower range than for observer JM; and DW's functions are perhaps more low-pass in form. The absolute values of DW's sensitivities for moving stimuli are systematically higher than those of the older observer, JM. As in the case of JM, DW's sensitivity for static gratings usually peaks at a lower spatial frequency than does that for moving gratings.

Fig. 3 summarizes the data for observers JM and DW: maximal sensitivity is shown as a function of eccentricity for the moving and stationary gratings. The estimate of maximal sensitivity was taken from the fitted curves of Figs. 2a and b, except in the few cases (static gratings at some high eccentricities) where only a single threshold was recorded: in these cases the corresponding sensitivity is plotted directly.

2.3. Discussion

Our measurements support the often-repeated claim of Exner that at the edge of the visual field there is a region where stationary objects are invisible but moving stimuli can be detected. However, Fig. 3 shows that the movement-sensitive region beyond 90° should not be thought of as unique: contrast sensitivity is falling concomitantly throughout the far periphery for both stationary and moving stimuli. There is no sense in which the extreme periphery is a region of enhanced sensitivity to motion, as is some-

times claimed: even for moving stimuli, sensitivity declines monotonically as eccentricity increases above 70°.

Formally, our experiment does not distinguish between sensitivity to motion and sensitivity to temporal modulation; and we note that temporal frequency varies as we vary the spatial frequency of our test bar. Our later experiments offer some evidence that the edge of the retina is sensitive to direction of motion. We also note that our mean stimulus luminance of 12 cd m^{-2}, although common in everyday conditions, may be effectively mesopic at an eccentricity of 90°, owing to the reduced level of light that reaches the retinal margin. The actual sensitivities of the rods and the large cones near the ora serrata are unknown, and also uncertain is the ray path by which light reaches this region, but between 70° and 90° the effective pupil area is reduced from 0.55 to 0.28 of its value for the line of sight (Jay, 1962). It is thus possible that the rod-cone balance changes over the range of eccentricities studied here.

3. Experiment 2

The purpose of Experiment 2 was to measure contrast sensitivity for different directions of moving stimuli in the extreme periphery. Drifting Gabor patches were presented near the limit of the visual field and contrast sensitivity thresholds were measured for 36 directions, from 5° to 355°, in increments of 10°. This experiment and the following one have been briefly reported in To and Mollon (2005).

3.1. Methods

3.1.1. Set-up

The observer's left eye was level with the centre of the display, which was located one meter away. The observer was required to place his or her head on a chin-rest located in front of a three-sided black booth (see Fig. 4, booth not shown), which served to minimize light scattered from the monitor into the rest of the visual field. A chin-rest stabilized the head. The right eye was covered by an eye-patch. To ensure that the observer maintained fixation on a central point while judging the peripheral stimuli, the fixation light was viewed through a long narrow tube, so that any alteration of eye position or rotation became apparent by the disappearance of the light. A protractor below the tube allowed the experimenter to adjust accurately the position of the light when testing for different eccentricities.

3.1.2. Stimuli

The visual stimuli were generated on a Sony FD Trinitron Colour Graphics 17-in. monitor (GDM-F400T9) using a Cambridge Research Systems VSG graphics card (VSG 2/5). The frame rate was 100 Hz. The targets for detection were Gabor patches with diameter 5.26° (σ = .75°; cut-off at 3.5σ from the centre). A black mask with an aperture subtending the diameter of the stimulus was added to the surrounding area. Within the fixed Gaussian patch, the sinusoidal component of 0.55 cycles per degree moved in a direction orthogonal to the grating at 2.78° s^{-1}. In the absence of modulation, the field had a luminance of 66 cd m^{-2}. Its color was gray (CIE 1931 *x*-, *y*-coordinates = .283, .311).

Observers were tested with Gabor patches drifting in 36 different drift directions, from 5° to 355° in increments of 10°. The convention for specifying drift direction is given in Fig. 5. The centre of the Gabor was located in the extreme periphery of the temporal field of the left eye.

3.1.3. Observers

Contrast sensitivity thresholds were collected from the authors, JDM and MT. Although both observers were myopic, neither was
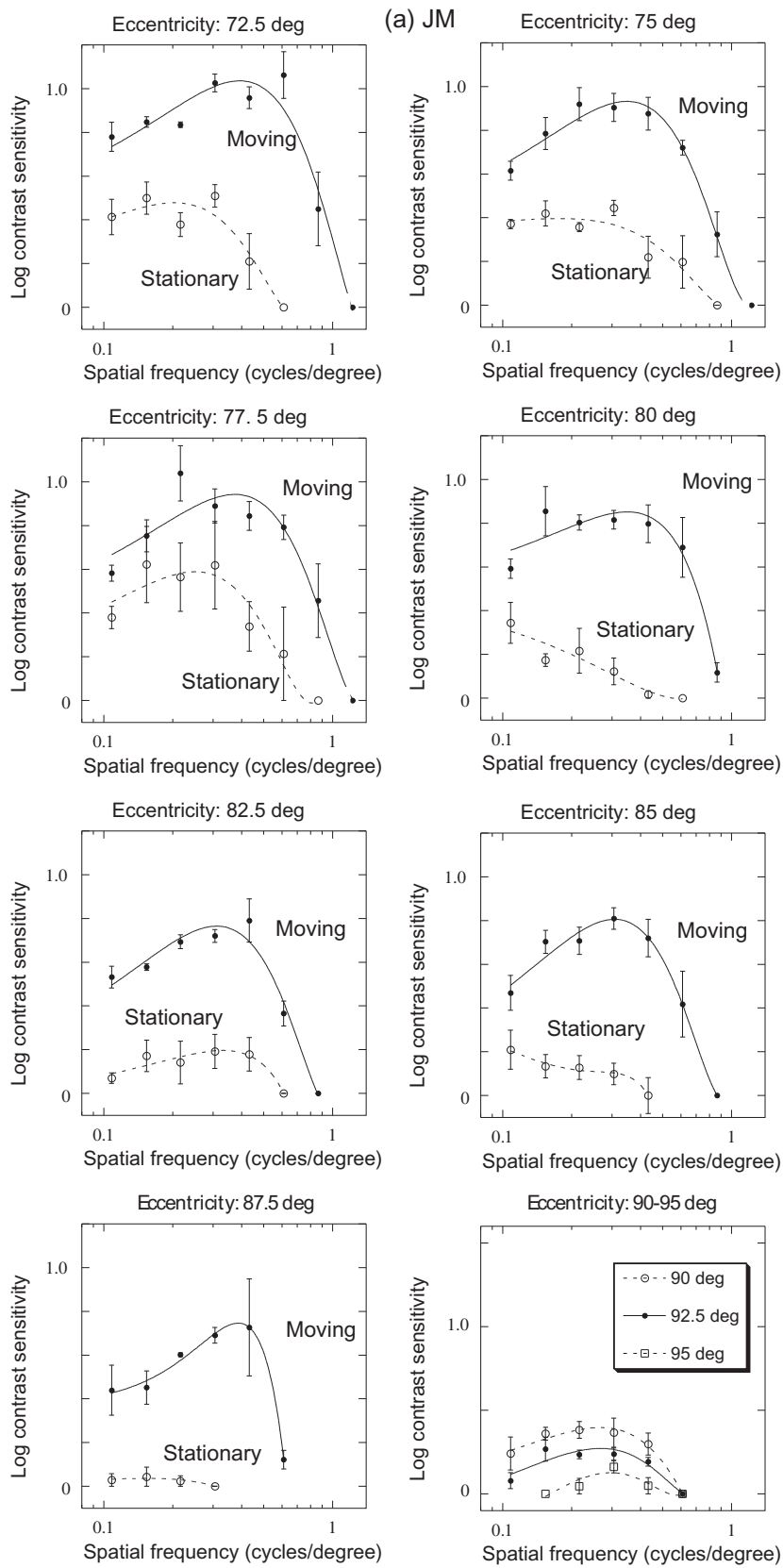
Fig. 2a. Spatial contrast sensitivity functions for JM for eccentricities 72.5–95°. In the first seven panels, the solid points represent log sensitivity to moving gratings and open circles represent sensitivity to static gratings. In the final panel, for the most extreme eccentricities, only sensitivities for moving gratings are shown. The fitted curves are third-order polynomials and have no theoretical significance. Error bars represent ±1 SEM, based on four independent runs.

visually corrected during testing, since the Gabors were of very low spatial frequency and since conventional contact lenses are not de-

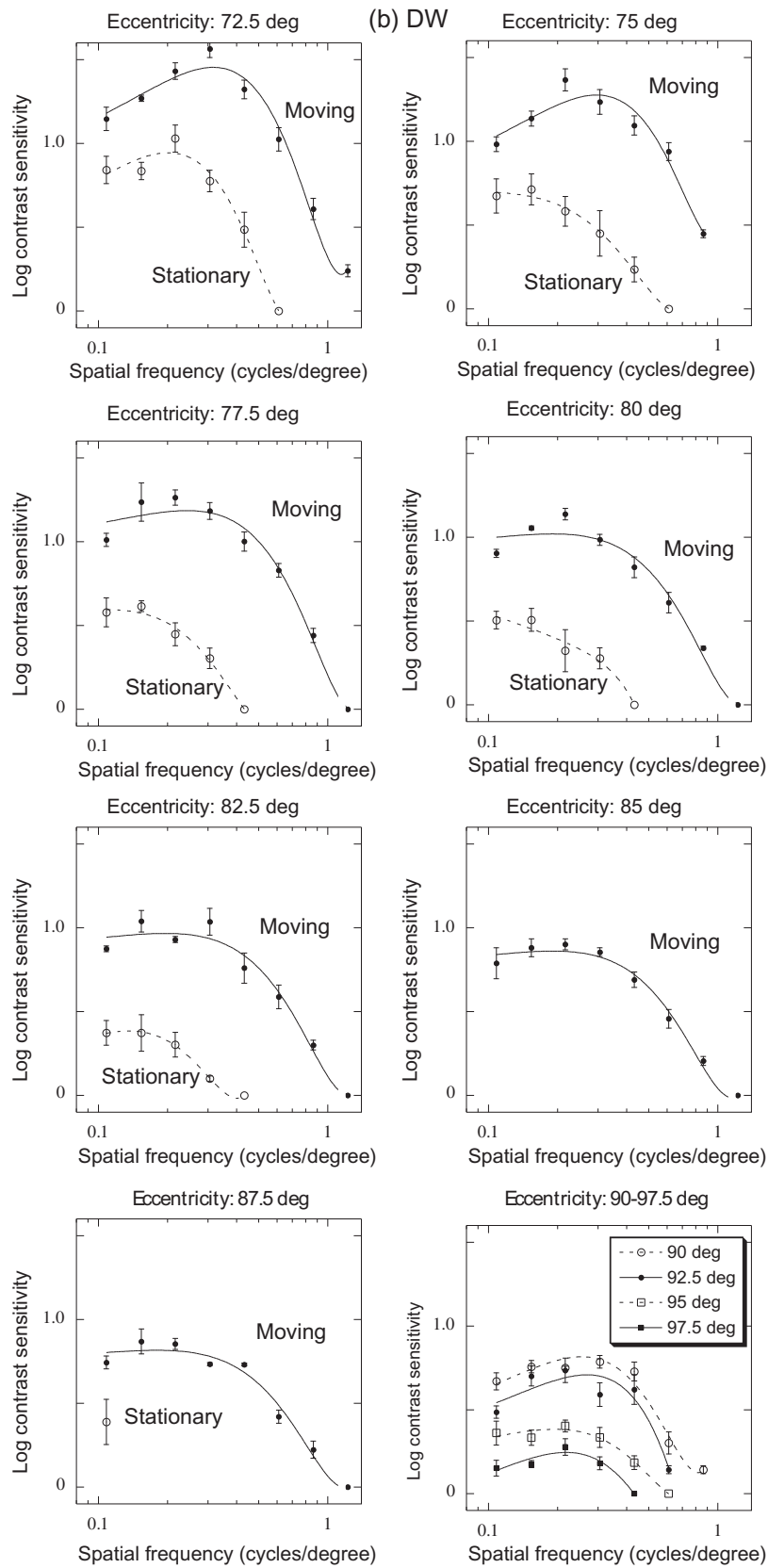signed to improve image quality in the region of 90° from the line of sight.

Fig. 2b. Spatial contrast sensitivity functions for DW for eccentricities 72.5–97.5°. Other details as for Fig. 2a.

3.1.4. Procedure

Contrast detection thresholds were measured using a two-interval temporal forced choice. Each trial was divided into two succes-sive observation intervals of ∼7 s. A short tone signalled the beginning of each interval. On each trial, the Gabor patch was presented randomly in one of the two intervals. The stimulus was
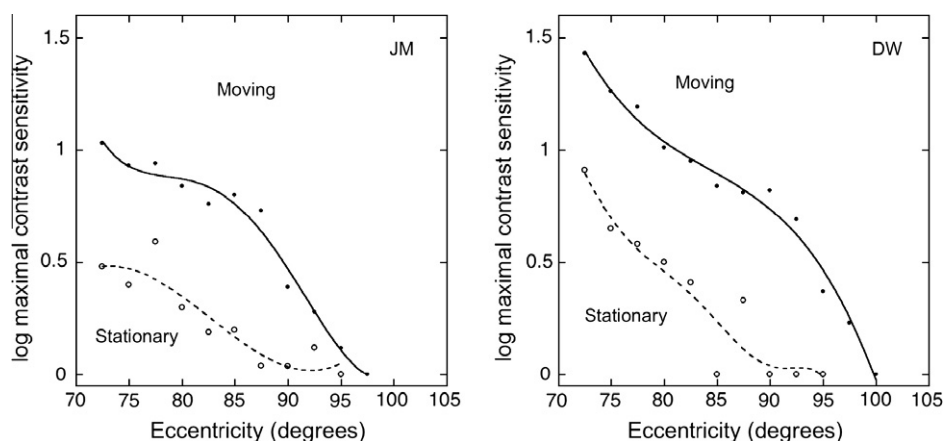
Fig. 3. Summary data for JM and DW: maximal sensitivity is shown as a function of eccentricity for the moving and stationary gratings. The estimate of maximal sensitivity was taken from the fitted curves of Figs. 2a and b, except in the few cases (static gratings at some high eccentricities) where only a single threshold was recorded: in these cases the corresponding sensitivity is plotted directly.
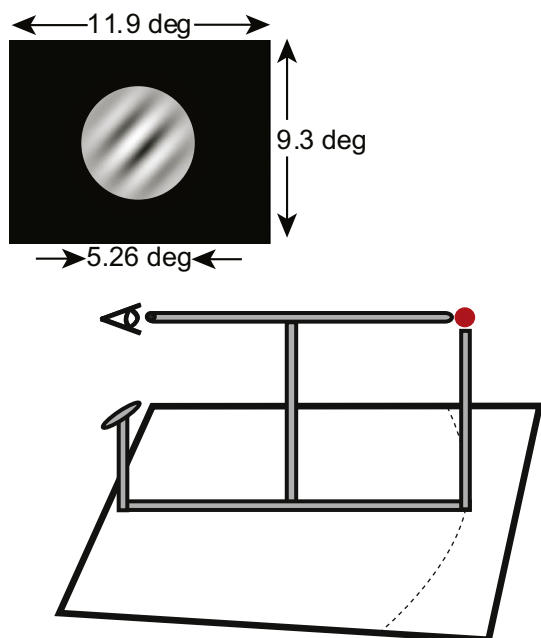

Fig. 4. Set-up for Experiments 2–4. Observers were seated with their left eye level with the center of a calibrated monitor, located one meter from the test eye. A chin-rest was used to stabilize head position. The observer viewed a fixation light through a long narrow tube, so that any displacement or rotation of the eye became apparent by the disappearance of the light.

presented within a 6.8 s Gaussian temporal envelope such that the maximal contrast was attained at 3.4 s from the start of each stimulus-displaying interval. The observer was asked to press one of two buttons to identify the interval containing the target. Auditory feedback was provided. The next trial was initiated by the observer's response.

Contrast sensitivities were calculated as the logarithms of the reciprocals of the contrast detection thresholds that were measured using a single staircase procedure, which converged to the 70.17% correct point. Contrast was set to 100% at the beginning of each staircase and was subsequently modified according to the observer's response. For the first two reversals in a block, contrast was decreased by a factor of 2 after two consecutive correct responses and increased by a factor of 2 after one incorrect response. After this, the staircase step size was either increased or decreased

by a factor of $2^{1/2}$. The threshold was taken as the mean of the test contrast for the final eight reversals after a total of 11 reversals.

3.1.5. Preliminary procedures and calibrations
3.1.5.1. Choice of spatial frequency. The measurements of Experiment 1 suggest that a spatial frequency of 0.3 cycles per degree would be optimal for the measurements. However, we were concerned by the fact that the presentation of a drifting Gabor patch is accompanied by modulations in mean luminance and that this cue might be used to identify the positive interval. The modulation of flux varies with spatial frequency: Gabors of higher spatial frequencies yield more stable output. These variations were computed for spatial frequencies ranging from 0.10 cycles per degree to 0.55 cycles per degree. In addition, direct empirical measurements were made using a photodiode placed 1 m from the centre of the monitor. As both calculations and direct measurements showed that luminous flux changes for drifting Gabor patches with a spatial frequency of 0.55 cycles per degree are less than 1%, this was chosen as the stimulus frequency.

3.1.5.2. Contrast for different orientations. It was essential for this experiment that Gabor patches of different orientations set to the same contrast value should produce the same luminance modulations. Potential asymmetries could arise from the horizontal scan of the raster or from the vertical arrangement of the phosphor lines on a Sony Trinitron screen. To check for asymmetries, the differences between the peaks and troughs of luminance generated by Gabors drifting in different directions were compared. The luminance fluctuations were similar for most orientations. Horizontally oriented Gabors drifting in directions 0° and 180° had slightly higher modulations, but these did not differ from the other orientations by more than 3.33%.

3.1.6. Locating the edge of the visual field
Before testing, observers performed preliminary detection tasks at various eccentricities to locate the limit of their visual field. The maximal eccentricities at which the observers could reliably set a threshold for all directions were 82.5° and 93.75° for JDM and MT respectively.

3.2. Results

JDM and MT completed a total of 72 and 288 staircases respectively: Two sets of contrast thresholds for 36 drift directions were obtained from JDM at 82.5° eccentricity and eight sets of contrast
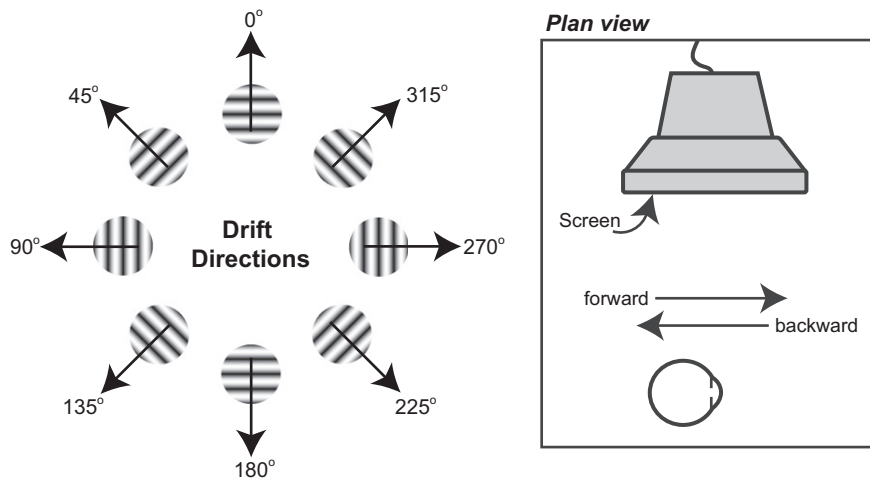
Fig. 5. *Left*: Convention for specifying direction of drift. *Right*: A plan view of the set-up showing that when the observer viewed with his or her left eye, 90° represented a literally backward direction, whereas 270° was a forward direction.

thresholds for 36 directions were obtained from MT at 90° and 93.75° eccentricity. The mean contrast thresholds for each eccentricity and drift direction are presented for observers JDM and MT in Fig. 6. For simplicity's sake, 82.5°, 90° and 93.75° eccentricity will be henceforth denoted by E82.5°, E90° and E93.75°, respectively.

Direction of drift had a significant effect on observers' thresholds: the effect was significant for JDM at E82.5° and MT at E90° and E93.75° $[F(35, 71) = 2.719, p < .005; F(35, 143) = 2.327, p < .0005; F(35, 143) = 5.761, p < .0001$, respectively]. Peak sensitivities were for directions near the cardinal axes, and minima were near the obliques. While this was the case for both observers, their 'preferred' and 'non-preferred' directions were somewhat different.

A computer simulation verified the significance of the shift in preferred directions from the cardinals in each observer. The pro-

gram fitted a 4-cycle sine wave through each observer's recorded thresholds and reported the actual shift of the data. In addition, the program generated 10,000 simulated threshold curves that were sampled from normal distributions with the actual thresholds and standard errors measured. Sine waves were then fitted through each curve and the mean phase from the simulations sample was computed, and the standard deviation of the distribution of the fitted phases was taken as a measure of confidence to determine how far the observed data were shifted from the cardinals.

Each sine wave fit was weighted in such a way as to minimize the chi-square value between the actual thresholds and the computer-generated ones. Although fitting sine waves assumed that the threshold maxima were located mid-way between the minima, this was not necessarily the case; however, the simulation was
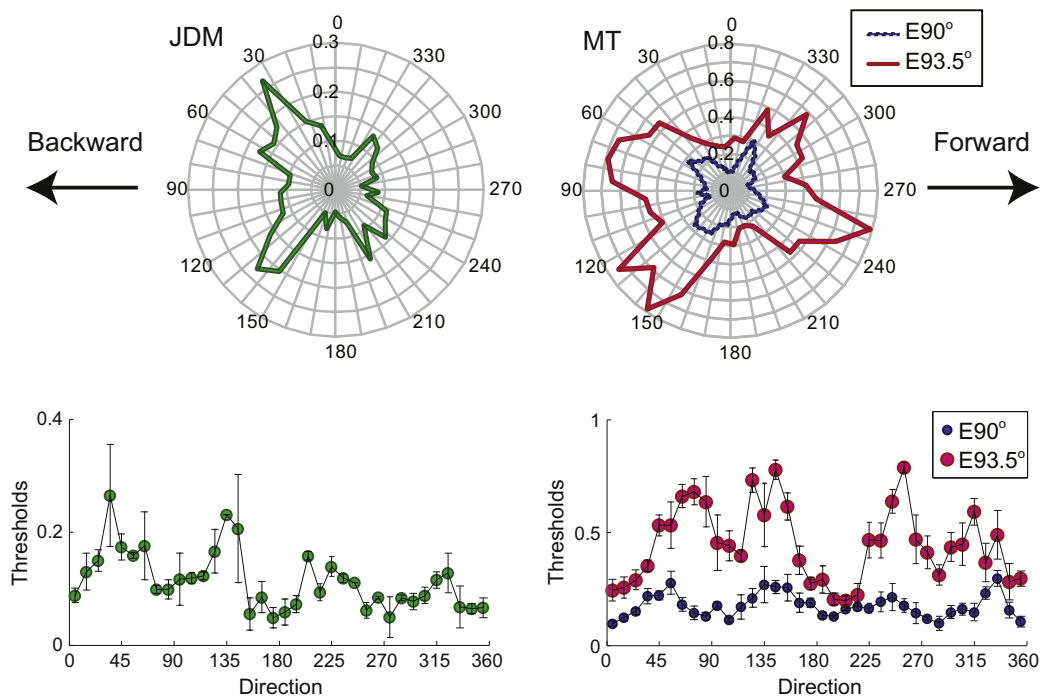

Fig. 6. Results from Experiment 2. Radial representation of mean contrast detection thresholds obtained from JDM at eccentricity E82.5° (top left) and those from MT at eccentricities E90° (top right; dashed) and E93.75° (top right; continuous) are shown in the top left and right panels respectively. The lower two panels present the same data in a linear graph with ±1 SEM based on two independent runs for JDM at eccentricity E82.5° (bottom left) and four independent runs each for MT at eccentricities E90° (bottom right; small) and E93.75° (bottom right; large).

useful in indicating whether there was a general shift in preferred directions in each observer and whether this shift would be significant in a 10,000 simulated trial.

JDM's thresholds collected at E82.5° were best fitted with a sine wave with an anti-clockwise phase shift of 4.07°. The simulation calculated a mean shift in 10,000 simulations of 4.16° ($\sigma = 1.74$, $p < .001$) in the same direction. MT's actual thresholds at E90° eccentricity were most accurately fitted with a sine wave shifted 9.49° in the clockwise direction, while the simulation computed an estimated mean phase shift of 9.45° ($\sigma = 1.81$, $p < .015$). Interestingly, the shift in MT's measured thresholds at E93.75° increased to 15.53° clockwise, agreeing with the estimated mean shift of 15.57 ($\sigma = 1.05$, $p < .025$) generated by the simulations. In all cases, the phase shifts were statistically significant.

Apart from the anisotropy described above, another prominent asymmetry in direction sensitivity was noted: observers were generally more sensitive to Gabor patches drifting in forward motions (directions 185–355°) compared to those drifting backwards (directions 5–185°). We refer to these directions as forward and backward (instead of centripetal and centrifugal) because our stimuli presented at the temporal edge of the visual field were not drifting towards or away the fovea but literally in forward and backward directions (see right panel in Fig. 5). The forward bias observed here reached significance for JDM at E82.5° [$F(1, 71) = 12.897$, $p < .001$] and MT at E93.75° [$F(1, 143) = 5.722$, $p < .02$], and was almost significant for MT at E90° [$F(1, 143) = 3.216$, $p = .075$].

4. Experiment 3

Adelson and Movshon (1982) introduced the use of drifting plaids in the study of motion. They superposed two moving gratings of different orientations and proposed that the speed and overall direction of the resultant plaid could be predicted by the intersection of the constraint lines of motion vectors that represented its two components. In addition, they suggested two stages of motion analysis for two-dimensional patterns: a lower level where the features of each component, such as speed, direction and orientation, were processed, and a higher level where these signals were integrated using the intersection of constraints.

In central vision, motion studies measuring coherence of plaids (Heeley & Buchanan-Smith, 1992) and resolution of direction of motion (Hupé & Rubin, 2004) show better performance for plaids drifting along the horizontal and vertical directions. Because the plaid patterns moving cardinally are composed of two oblique gratings, the findings suggested that the anisotropies originated at the second stage of motion processing, where information from the two component gratings is integrated.

Experiment 3 investigated the origins of the anisotropy found in Experiment 2 by measuring contrast sensitivity for Gabor and plaid stimuli presented at high eccentricities. Instead of using the four classical cardinal directions and corresponding intermediate directions, we used the preferred and non-preferred directions previously collected from observers JDM and MT. If the directions of maximal and minimal thresholds for Gabors matched those for plaids, this would suggest that the directional anisotropy arises more centrally in the visual pathway, after the plaid components have been integrated. On the other hand, if the maximal thresholds for the Gabors coincided with the minimal thresholds for the plaids, then this would imply that the anisotropy arises earlier in the pathway, where the direction of each component is processed separately.

4.1. Methods

The methods in Experiment 3 were similar to those of Experiment 2 and the observers were the same. Contrast sensitivity was measured in only eight directions of motion, which corresponded to

the observers' individual preferred and non-preferred directions as established in Experiment 2: for JDM these were −5°, 85°, 175°, 265° and 40°, 130°, 220°, 310° at eccentricity E82.5°, and for MT they were 15°, 105°, 195°, 285° and 60°, 150°, 240°, 330° at eccentricity E93.75°. Two types of stimulus were used in different, randomly interleaved sessions. In the Gabor condition, the target was the Gabor patch used in Experiment 2 (with a spatial frequency of 0.55 cycles per degree and drifting at 2.78 cycles per second); in the Plaid condition, the target was constructed by superposing two perpendicular Gabor patches identical to those of the Gabor condition and drifting in either two preferred or two non-preferred directions. Because preferred directions were perpendicular and non-preferred directions were situated mid-way in between, a plaid composed of two Gabor patches drifting in non-preferred directions appeared to follow a preferred direction, and vice versa; see Fig. 7.

4.2. Results

Observers JDM and MT each completed a total of 64 staircases: four sets of contrast thresholds were obtained from each Gabor and Plaid condition. Mean contrast thresholds are shown in Fig. 8, where circles and triangles represent Gabor and Plaid conditions respectively. As in Experiment 2, results from the Gabor condition revealed a significant effect of direction of drift on thresholds [$F(7, 31) = 7.537$, $p < .0001$ for JDM and $F(7, 31) = 4.737$, $p < .005$ for MT] and the anisotropies were similar, with minimal thresholds for the original preferred directions [$F(1, 31) = 13.546$, $p < .001$ for JDM and $F(1, 31) = 23,735$, $p < .0001$ for MT]. In the Plaid condition, drift direction also had a significant effect on thresholds [$F(7, 31) = 10.838$, $p < .00001$ for JDM and $F(7, 31) = 6.555$, $p < .0005$ for MT]; and the differences in thresholds between preferred and non-preferred directions were very significant [$F(1, 31) = 43.516$, $p < .00001$ for JDM and $F(1, 31) = 28,768$, $p < .0001$ for MT]. However, results for preferred and non-preferred directions were reversed: detection thresholds for plaids drifting in preferred directions were now the higher and those for non-preferred directions were now the lower [$F(1, 63) = 54.968$, $p < .00001$ and $F(1, 63) = 52.279$, $p < .00001$]. The correlations between thresholds for Gabor and for plaid stimuli were −0.71 and −0.85 for JDM and MT respectively: the maximal thresholds for the Gabors coincided with the minimal thresholds for the plaids, and vice versa. This suggests that the anisotropy arises at a low level in the visual system. As a control, observer MT repeated the experiment in the central field; in this case, there were no significant differences between thresholds for different directions [$F(7, 31) = 0.76$, $p = .63$] and no differences between Gabor and Plaid conditions [$F(1, 31) = 3.97$, $p = .06$]. This control suggests that the present effects are specific to the far periphery.

5. Experiment 4

In the preceding experiments, we recorded only detection thresholds for moving stimuli. In a final experiment we measured thresholds for discriminating the direction of motion.
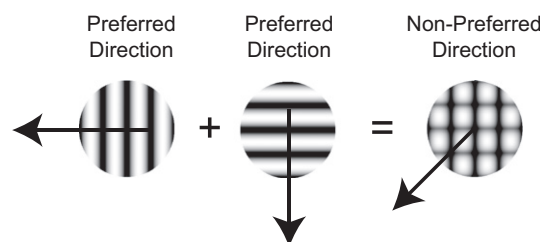

Fig. 7. Motion of plaids. The superposition of two Gabors drifting in preferred directions results in a plaid moving in a non-preferred direction.
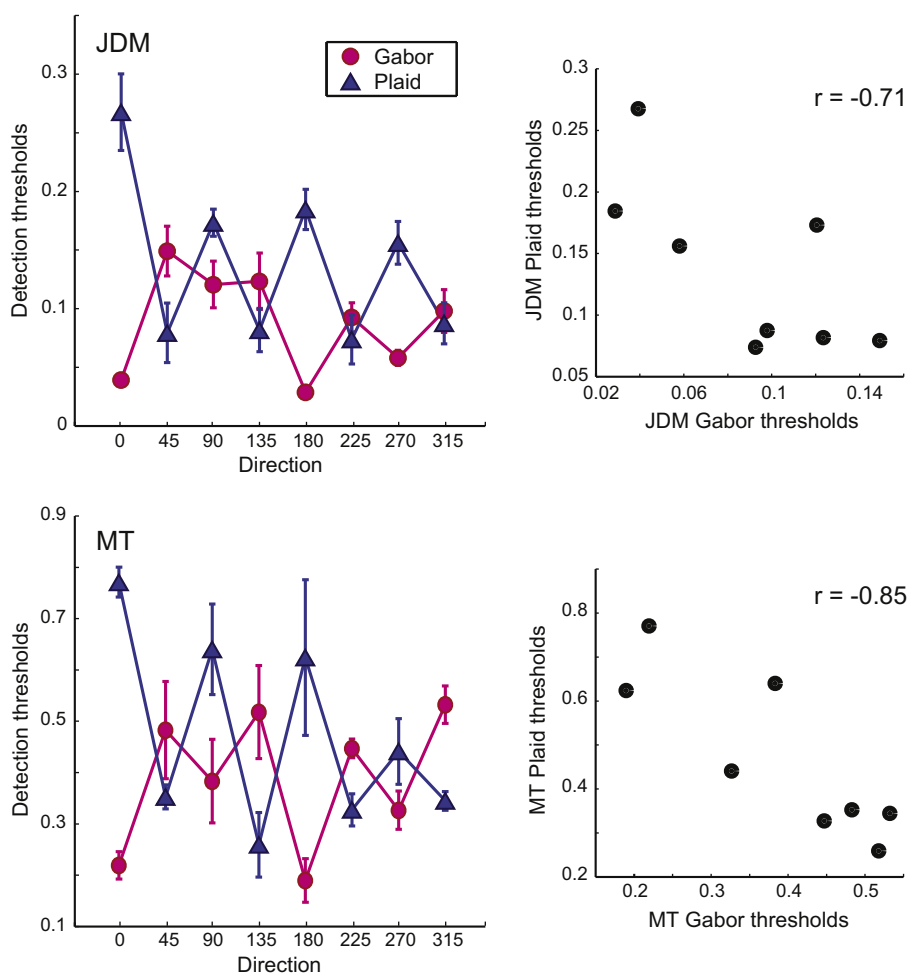
Fig. 8. Results from Experiment 3. On the left, mean contrast thresholds are shown for Gabor and plaid patches from observers JDM at eccentricity 82.75° (top) and MT at eccentricity 93.75° (bottom). Mean thresholds for Gabor and plaid stimuli are represented by circles and triangles. Errors are ±1 SEM based on four independent runs. On the right, Plaid thresholds are plotted against Gabor thresholds. The data show a strong negative correlation between the two thresholds: −0.71 for JDM (top) and −0.85 for MT (bottom).

5.1. Methods

The stimuli were Gabors as in Experiment 2 and the same experimental set-up was used. For eight references directions, we estimated how far a second stimulus had to differ in direction of motion for correct discrimination. Thresholds were measured by two-interval temporal forced choice. Each trial was divided into two successive intervals. A short tone signalled the beginning of each interval. On each trial, two Gabors were presented: in one interval, the target drifted in the reference direction and in the other, the target drifted in a direction that was adjusted according to the observer's accuracy. Each stimulus was presented within a 6.8 s Gaussian temporal envelope such that the maximal contrast was attained 3.4 s after the interval started.

The interval containing the reference Gabor was randomized, and the observer was asked to identify this interval by pushbuttons. Auditory feedback was given. Variable Gabors that differed in clockwise and counter-clockwise directions were tested in separate blocks. The reference direction was also blocked, giving a total of 16 conditions, each of which was repeated four times in separate sessions.

Discrimination thresholds were calculated using a single staircase procedure, which converged to the 70.17% correct point. At the beginning of each staircase, the variable target direction was 90° offset from the reference direction, and its direction was there-

after modified according to the observer's accuracy. Since the starting point of the staircase differs by 90° from the reference direction, the observer must at this point judge direction of motion, and not merely orientation, if the staircase is to proceed. For the first two reversals in a block, the difference between target and test directions was decreased by a factor of 2 after two consecutive correct responses and increased by a factor of 2 after one incorrect response. Thereafter, the staircase step size was either increased or decreased by a factor of $2^{1/2}$. The threshold was taken as the mean value for the final eight reversals after a total of 11 reversals.

The observers were the authors MT and JM, plus a third female observer, RS who was naïve as to the purpose of the experiment. They were tested at eccentricities E90°, E87.5° and E85° respectively.

5.2. Results and discussion

Fig. 9 shows for each observer the mean thresholds for eight directions of motions. A repeated measures ANOVA, with the factors Reference Direction and Clockwise/Counter-clockwise Threshold, shows a significant main effect of direction [$F[7, 186] = 10.51$, $p < .01$]: discrimination thresholds are generally lowest for upward and downward motion, where the absolute values are under 20°. There was a significant interaction between Clockwise/Counter-clockwise Threshold and Observer [$F(2, 9) = 5.43$, $p < .05$].
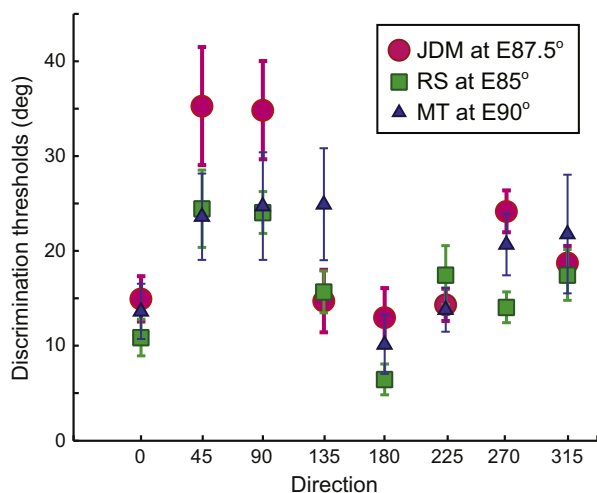
Fig. 9. Mean direction discrimination thresholds from Experiment 4. Different symbols represent data from individual observers: JDM at E87.5° eccentricity (circles), RS at E82.5° (squares) and MT at E90° (triangles). Errors are ±2 SEM based on eight independent estimates of each threshold (four clockwise and four counterclockwise estimates).

To perform this task, the observer must do more than detect a Gabor at the edge of vision: he or she must have information either about its orientation or its direction of motion. Observers reported clear sensations of motion direction, and certainly, to initiate the staircase (which was always possible) they could not rely simply on the orientation of the Gabor.

6. General discussion

The aim of this study has been to offer a preliminary psychophysical characterization of vision at the temporal edge of the field. Experiment 1 showed that contrast sensitivity is better for moving than for stationary gratings over a range of eccentricities in the far periphery. It is true that there is a region at the edge of the field where only moving stimuli can be detected, but this region should be seen in the context of a larger region from eccentricities of 70° outwards. Throughout the far periphery, contrast thresholds for moving and stationary stimuli are rising concomitantly. There is no evidence that the far periphery enjoys a motion sensitivity superior to that of central vision; and in this respect our results are concordant with the conclusion drawn by Finlay (1982). In the fovea, at low spatial frequencies such as used in our present experiments, Robson (1966) classically showed that sensitivity is much higher for a stimulus modulated at 6 Hz than for a stimulus modulated at 1 Hz. Our argument is not that the extreme periphery contains a special mechanism for detecting temporal modulation or motion; it is rather that few of the other channels of central vision extend to the extreme edge of the retina.

Experiment 2 measured contrast detection thresholds for Gabor patches drifting in different directions at the edge of the visual field and revealed anisotropies in directional preference. Firstly, there were four peaks in contrast sensitivity, for stimuli moving in near-cardinal directions. Secondly, sensitivity for motion in forward directions was higher than for backward ones.

In Experiment 3, contrast sensitivity thresholds collected from Gabor and Plaid conditions showed strong but complementary anisotropies: In agreement with Experiment 2, minimal thresholds were recorded for the Gabor stimulus drifting in near-cardinal directions, but minimal thresholds for the plaid stimulus were located along the observers' non-preferred oblique directions.

Experiments 1–3 measure only detection thresholds and so show only the sensitivity of the extreme periphery to temporal

modulation. The observed anisotropies might be held to reflect variations in orientation sensitivity. However, two of our results imply a sensitivity to direction of motion: (i) in Experiments 2 and 3, we found greater sensitivity to Gabors drifting forwards than to Gabors drifting backwards, and (ii) in Experiment 4, observers showed at least a coarse discrimination between opposite directions of motion.

6.1. Origin of anisotropies in the detection of drifting Gabors

The increased sensitivity for movement along two orthogonal axes – observed in both Experiments 2 and 3 – suggests that the anisotropy has a neural basis and does not result from optical factors: Whereas a single anisotropy could easily be explained by optical factors, such as astigmatism (e.g. Leibowitz, Johnson, & Isabelle, 1972) or the diffraction patterns resulting from the slit-like pupil aperture or the chromatic dispersion that affects rays refracted at the edge of the cornea, it is difficult to envisage how these could give enhanced sensitivity for two orthogonal axes at the expense of the obliques.

In Experiment 3, the complementarity of preferred directions in the Gabor and Plaid conditions suggested that the anisotropy in direction selectivity arises at the early stages of visual processing. Because plaids drifting in a non-preferred direction were composed of two Gabors drifting in a preferred direction, these results showed that the optimal directions for the plaid stimulus were determined by those of its components. This finding contrasts with what has been reported for foveal vision (Heeley & Buchanan-Smith, 1992; Hupé & Rubin, 2004) and is compatible with the possibility that the anisotropy at the edge of the visual field has its origin at the level of retinal ganglion cells (see below).

6.2. The bias for forward motion

The increased sensitivity for forward directions that we find at the very edge of the visual field is comparable to the centripetal bias reported in less eccentric viewings. A general preference for movement towards the fovea has been supported both in psychophysical (Edwards & Badcock, 1993; Koenderink et al., 1978; Lisberger & Westbrook, 1985; Mateeff & Hohnsbein, 1988; Raymond, 1994; Tychsen & Lisberger, 1986) and physiological (Motter, Steinmetz, Duffy, & Mountcastle, 1987; Steinmetz, Motter, Duffy, & Mountcastle, 1987) research.

The superior performance that we observe for forward motion over backward motion could either reflect a hard-wired property of the visual apparatus or could arise from long-term adaptation during everyday experience. We consider these two possibilities in turn:

(i) In the rabbit retina, within a region corresponding to the central 40° of the visual field, ON–OFF cells with a preference for centripetal/forward motion are twice as common as those preferring centrifugal/backward motion (Oyster, 1968; Oyster & Barlow, 1967). In terms of the geometry of optic flow during locomotion, the central 40° for the laterally-placed eye of the rabbit corresponds to the far temporal periphery for human vision. It is possible that the human peripheral retina, like that of the rabbit, has an excess of detectors for centripetal/forward motion.

(ii) Alternatively, the bias to forward motion found in Experiments 2 and 3 could be the result of a contrast gain control mechanism. Forward navigation produces continuous expanding optic flow patterns, comparable to our backward-drifting Gabors. The contrast gain that we envisage would be similar to that underlying the horizontal effect (Essock, DeFord, Hansen, & Sinai, 2003; Hansen & Essock, 2004; Wainwright, Schwarts, & Simoncelli, 2001) and the

inverse oblique effect (Wilson, Loffler, Wilkinson, & Thistlethwaite, 2001). The mechanism would work by amplifying sensitivity for infrequent directions while dampening sensitivity for frequent ones, thus allowing infrequent features to stand out (Keil & Cristobal, 2000; Scott, Lavender, McWhirt, & Powell, 1966; Switkes, Mayer, & Sloan, 1978). Forward/centripetal patterns usually signal unpredicted events, such as imbalance of posture or the approach of an object from the periphery.

6.3. A single type of ganglion cell at the retina edge?

Polyak (1941) reports that the ganglion cells of the extreme periphery occur in small groups (of 'twos or threes') with large spaces between. It is attractive to postulate that these ganglion cells might be of a single, motion-sensitive type and that each local group contains cells with different preferred directions.

The results of Experiments 2 and 3 would suggest the presence in the extreme periphery of cells analogous to the ON–OFF type of directionally-selective ganglion cell found in the rabbit retina (Barlow & Hill, 1963; Oyster, 1968; Oyster & Barlow, 1967). Traditionally it has been held that directionally-selective ganglion cells do not occur in the primate retina, but Dacey et al. (2003) has identified the recursive monostratified and recursive bistratified types as possibly directionally selective (see also Yamada et al., 2005). The monostratified type would correspond to the ON-type directionally-selective cells of Barlow and Hill and the bistratified – since their dendritic fields ramify in both the ON and OFF strata of the inner plexiform layer – would correspond to the ON–OFF type. If, as we suggest, directionally-selective cells are present at the edge of the human retina, they are more likely to be of the ON–OFF type than of the ON type. In the study of Oyster and Barlow, whereas the ON-type fell into three groups according to their preferred directions, the ON–OFF cells fell into four groups, a grouping concordant with our own results. The four preferred directions of the rabbit ON–OFF ganglion cells were aligned approximately (but not exactly) with the four cardinal directions, much as we found for our psychophysical observers. Moreover, in non-primate mammals, the ON–OFF directionally-selective retinal ganglion cells project to the geniculostriate pathway (and to the superior colliculus) whereas the main projection of the ON type is to the accessory optic system (Rodieck, 1998, pp. 319–325).

Our prediction would be that directionally-selective ganglion cells – probably, but not necessarily, of the ON–OFF type – will be found in the extreme periphery of the primate and human retina. At first sight, our results might be thought to require these ganglion cells to occur in groups of four rather than Polyak's 'twos or threes'. In so far as the ganglion cells occur in pairs, one possibility is that the members of each pair are selective for opposite directions and are opponently linked. We may also expect to find, perhaps, paired starburst amacrine cells with dendritic fields that are spatially offset but overlapping: The overlapping dendrites of such pairs are known to exert reciprocal inhibition on each other (Euler & Hausselt, 2008; Lee & Zhou, 2006). The extreme peripheral retina offers the histologist an attractive opportunity: The possibility of examining a single retinal circuit in isolation from the plurality of other circuits that are intermingled in central retina.

6.4. A practical note

The modern equivalent of a predator entering our temporal field is an automobile overtaking us on our offside. There is a current fashion for spectacle frames that have temples diverging to form a very broad junction with the front frame. Such temples necessarily occlude the far periphery of the retina and we suggest that they may increase the risk of accidents. Such warnings have been made in the past, at times when broad temples have been fashionable (Taylor, 1964); and the restriction of the field has been shown perimetrically (Ruffell Smith & Weale, 1966; Steel, Mackie, & Walsh, 1996).

Acknowledgments

References

Adelson, E. H., & Movshon, J. A. (1982). Phenomenal coherence of moving visual patterns. *Nature, 300*(5892), 523–525.

Azzopardi, P., & Cowey, A. (1998). Blindsight and visual awareness. *Consciousness and Cognition, 7*(3), 292–311.

Barlow, H. B., & Hill, R. M. (1963). Selective sensitivity to direction of movement in ganglion cells of the rabbit retina. *Science, 139*, 412–414.

Bessou, M., Severac Cauquil, A., Dupui, P., Montoya, R., & Bessou, P. (1999). Specificity of the monocular crescents of the visual field in postural control. *Comptes Rendus de l'Académie des Sciences. Serie III, Sciences de la Vie, 322*(9), 749–757.

Brandt, T., Dichgans, J., & Koenig, E. (1973). Differential effects of central versus peripheral vision on egocentric and exocentric motion perception. *Experimental Brain Research, 16*(5), 476–491.

Crook, J. D., Peterson, B. B., Packer, O. S., Robinson, F. R., Gamlin, P. D., Troy, J. B., et al. (2008). The smooth monostratified ganglion cell: Evidence for spatial diversity in the Y-cell pathway to the lateral geniculate nucleus and superior colliculus in the macaque monkey. *Journal of Neuroscience, 28*(48), 12654–12671.

Dacey, D. M., Peterson, B. B., Robinson, F. R., & Gamlin, P. D. (2003). Fireworks in the primate retina: In vitro photodynamics reveals diverse LGN-projecting ganglion cell types. *Neuron, 37*(1), 15–27.

Druault, A. (1898). Note sur la situation des images rétiniennes formées par les rayons très obliques sur l'axe optique. *Archives d'Ophtalmologie, 20*, 685–692.

Edwards, M., & Badcock, D. R. (1993). Asymmetries in the sensitivity to motion in depth: A centripetal bias. *Perception, 22*(9), 1013–1023.

Essock, E. A., DeFord, J. K., Hansen, B. C., & Sinai, M. J. (2003). Oblique stimuli are seen best (not worst!) in naturalistic broad-band stimuli: A horizontal effect. *Vision Research, 43*(12), 1329–1335.

Euler, T., & Hausselt, S. E. (2008). Direction-selective cells. In A. I. Basbaum, A. Kaneko, G. M. Shepherd, & & G. Westheimer (Eds.). *The senses – A comprehensive reference* (Vol. 1, pp. 413–422). San Diego: Academic Press.

Exner, S. (1875). Uber das Sehen von Bewegungen und die Theorie des zusammengesetzen Auges. *Sitzungsberichte der Kaiserlichen Akademie der Wissenschaften, Wien, 72*, 156–190.

Finlay, D. (1982). Motion perception in the peripheral visual field. *Perception, 11*(4), 457–462.

Gibson, J. J. (1947). Motion picture testing and research. *Army Air Force Aviation Psychology Reports, 7*.

Greeff, R. (1900). Mikroscopische Anatomie der Sehnerven und der Netzhaut. In A. von Graefe & T. Saemisch (Eds.), *Handbuch der gesamten Augenheilkunde*. Berlin: Springer.

Grindley, G. C. (1942). *Notes on the perception of movement in relation to the problem of landing an aeroplane. Report FPRC 426*. Air Ministry Flying Personnel Research Committee.

Hansen, B. C., & Essock, E. A. (2004). A horizontal bias in human visual processing of orientation and its correspondence to the structural components of natural scenes. *Journal of Vision, 4*(12), 1044–1060.

Hartridge, H. (1919). The limit to peripheral vision. *Journal of Physiology (London), 53*, xvii–xviii.

Heeley, D. W., & Buchanan-Smith, H. M. (1992). Directional acuity for drifting plaids. *Vision Research, 32*(1), 97–104.

Hulk, J., & Rempt, F. (1984). Optokinetic sensations evoked by local stimulation of the peripheral retina. *Documenta Ophthalmologica, 56*(3), 237–242.

Hupé, J. M., & Rubin, N. (2004). The oblique plaid effect. *Vision Research, 44*(5), 489–500.

Jay, B. S. (1962). The effective pupillary area at varying perimetric angles. *Vision Research, 1*, 418–424.

Keil, M. S., & Cristobal, G. (2000). Separating the chaff from the wheat: Possible origins of the oblique effect. *Journal of the Optical Society of America A. Optics Image Science and Vision, 17*(4), 697–710.

Koenderink, J. J., Bouman, M. A., Bueno de Mesquita, A. E., & Slappendel, S. (1978). Perimetry of contrast detection thresholds of moving spatial sine patterns. II.

The far peripheral visual field (eccentricity 0 degrees–50 degrees). *Journal of the Optical Society of America, 68*(6), 850–854.

Lee, S., & Zhou, Z. J. (2006). The synaptic mechanism of direction selectivity in distal processes of starburst amacrine cells. *Neuron, 51*(6), 787–799.

Leibowitz, H. W., Johnson, C. A., & Isabelle, E. (1972). Peripheral motion detection and refractive error. *Science, 177*(55), 1207–1208.

Lisberger, S. G., & Westbrook, L. E. (1985). Properties of visual inputs that initiate horizontal smooth pursuit eye movements in monkeys. *Journal of Neuroscience, 5*(6), 1662–1673.

Mateeff, S., & Hohnsbein, J. (1988). Perceptual latencies are shorter for motion towards the fovea than for motion away. *Vision Research, 28*(6), 711–719.

McKee, S. P., & Nakayama, K. (1984). The detection of motion in the peripheral visual field. *Vision Research, 24*(1), 25–32.

Mollon, J. D., & Regan, B. C. (1999). Vision out of the corner of the eye. *Perception, 28*(Suppl.), 28.

Mollon, J. D., Regan, B. C., & Bowmaker, J. K. (1998). What is the function of the cone-rich rim of the retina? *Eye (London, 12*(Pt 3b), 548–552.

Motter, B. C., Steinmetz, M. A., Duffy, C. J., & Mountcastle, V. B. (1987). Functional properties of parietal visual neurons: Mechanisms of directionality along a single axis. *Journal of Neuroscience, 7*(1), 154–176.

Navarro, R., Artal, P., & Williams, D. R. (1993). Modulation transfer of the human eye as a function of retinal eccentricity. *Journal of the Optical Society of America A, 10*(2), 201–212.

Noorlander, C., Koenderink, J. J., den Ouden, R. J., & Edens, B. W. (1983). Sensitivity to spatiotemporal colour contrast in the peripheral visual field. *Vision Research, 23*, 1–11.

Oyster, C. W. (1968). The analysis of image motion by the rabbit retina. *Journal of Physiology, 199*(3), 613–635.

Oyster, C. W., & Barlow, H. B. (1967). Direction-selective units in rabbit retina: Distribution of preferred directions. *Science, 155*(764), 841–842.

Palmer, S. M., & Rosa, M. G. (2006). A distinct anatomical network of cortical areas for analysis of motion in far peripheral vision. *European Journal of Neuroscience, 24*(8), 2389–2405.

Pavard, B., Berthoz, A., & Lestienne, F. (1976). Rôle de la vision périphérique dans l'évaluation du mouvement linéaire, interaction visuo-vestibulaire et effets posturaux. *Le Travail Humain, 39*, 115–138.

Pointer, J. S., & Hess, R. F. (1989). The contrast sensitivity gradient across the human visual field: With emphasis on the low spatial frequency range. *Vision Research, 29*(9), 1133–1151.

Polyak, S. L. (1941). *The retina*. Chicago: University of Chicago Press.

Porter, T. C. (1902). Contributions to the study of flicker. II. *Proceedings of the Royal Society of London Series A, 70*, 313–329.

Purkinje, J. (1825). *Beobachtungen und Versuche zur Physiologie der Sinne: Neue Beiträge zur Kenntnis des Sehens in subjectiver Hinsicht*. Berlin: Reimer.

Raymond, J. E. (1994). Directional anisotropy of motion sensitivity across the visual field. *Vision Research, 34*(8), 1029–1037.

Riddoch, G. (1917). Dissociation of visual perceptions due to occipital injuries, with especial reference to appreciation of movement. *Brain, 40*, 15–57.

Robson, J. G. (1966). Spatial and temporal contrast sensitivity functions of the visual system. *Journal of the Optical Society of America, 56*, 1141–1142.

Robson, J. G., & Graham, N. (1981). Probability summation and regional variation in contrast sensitivity across the visual field. *Vision Research, 21*(3), 409–418.

Rodieck, R. W. (1998). *The first steps in seeing*. Sunderland, MA: Sinauer Associates.

Ruffell Smith, H. P., & Weale, R. A. (1966). Obstruction of vehicle-driver's vision by spectacle frames. *British Medical Journal, 2*, 445–447.

Scott, T. R., Lavender, A. D., McWhirt, R. A., & Powell, D. A. (1966). Directional asymmetry of motion aftereffect. *Journal of Experimental Psychology, 71*(6), 806–815.

Sharpe, C. R. (1974). The contrast sensitivity of the peripheral visual field to drifting sinusoidal gratings. *Vision Research, 14*(9), 905–906.

Steel, S. E., Mackie, S. W., & Walsh, G. (1996). Visual field defects due to spectacle frames: Their prediction and relationship to UK driving standards. *Ophthalmic and Physiological Optics, 16*(2), 95–100.

Steinmetz, M. A., Motter, B. C., Duffy, C. J., & Mountcastle, V. B. (1987). Functional properties of parietal visual neurons: Radial organization of directionalities within the visual field. *Journal of Neuroscience, 7*(1), 177–191.

Switkes, E., Mayer, M. J., & Sloan, J. A. (1978). Spatial frequency analysis of the visual environment: Anisotropy and the carpentered environment hypothesis. *Vision Research, 18*(10), 1393–1399.

Taylor, G. F. (1964). Dangerous spectacle frames. *British Medical Journal, 2*, 1597.

To, M., & Mollon, J. D. (2005). Anisotropy of motion sensitivity at the temporal margin of the visual field. *Perception, 34* (ECVP Abstract Supplement).

Tychsen, L., & Lisberger, S. G. (1986). Visual motion processing for the initiation of smooth-pursuit eye movements in humans. *Journal of Neurophysiology, 56*(4), 953–968.

van Ness, F. L., Koenderink, J. J., Nas, H., & Bouman, M. A. (1967). Spatiotemporal modulation transfer in the human eye. *Journal of the Optical Society of America, 57*(9), 1082–1088.

Wainwright, M. J., Schwarts, O., & Simoncelli, E. P. (2001). Natural image statistics and divisive normalization: Modeling nonlinearity and adaptation in cortical neurons. In M. Lewicki (Ed.), *Statistical theories of the brain*. Cambridge, MA: MIT Press.

Wetherill, G. B., & Levitt, H. (1965). Sequential estimation of points on a psychometric function. *British Journal of Mathematical and Statistical Psychology, 18*, 1–10.

Williams, R. W. (1991). The human retina has a cone-enriched rim. *Visual Neuroscience, 6*(4), 403–406.

Wilson, H. R., Loffler, G., Wilkinson, F., & Thistlethwaite, W. A. (2001). An inverse oblique effect in human vision. *Vision Research, 41*(14), 1749–1753.

Yamada, E. S., Bordt, A. S., & Marshak, D. W. (2005). Wide-field ganglion cells in macaque retinas. *Visual Neuroscience, 22*(4), 383–393.

Young, T. (1801). On the mechanism of the eye. *Philosophical Transactions of the Royal Society, 91*, 23–88.